Exploring Nanoscale Thermal Properties by integrating Scanning thermal microscopy with Inverse Methods.

Nathaly CHAARAOUI*, Nathalie TRANNOY*, Thierry DUVAUT

[1]University of Reims Champagne-Ardenne, IThEMM, Moulin de la Housse, BP 1039, 51687 Reims Cedex 2, France
*(nathaly.chaaraoui@univ-reims.fr, nathalie.trannoy@univ-reims.fr)

Abstract

The article aims to determine thermal conductivities for SiO2 at the nanoscale, using a Wollaston microprobe in Scanning Thermal Microscopy. Through experimental measurements and Finite Element Method modeling, the research strives to determine precise thermal conductivity values across varying SiO2 thicknesses. The Levenberg-Marquardt algorithm enhances accuracy in thermal conductivity determination, providing significant perspectives into nanoscale heat conduction properties and advancing our understanding of material behavior.

Nomenclature

$h_{equivalent}$: Equivalent heat transfer through the probe holder (W/m^2. K)
$h_{convectif}$: Convective heat transfer with the surrounding (W/m^2. K)
k: Thermal conductivity, (W/m.K)
Ip_c: Probe current in contact mode, (mA)
Ip_{wc}: Probe Current out of contact mode, (mA)
P_c: Dissipated power in contact mode, (W)
P_{wc}: Dissipated power out of contact mode, (W)
$R_{Pt/Rh}$: Resistance of Platine-Rhodium filament, (Ω)
T_a : Ambient temperature (K)
$Vout_c$: Probe voltage in contact mode, (V)
$Vout_{wc}$: Probe voltage out of contact mode, (V)
ΔP: Electrical power difference, (W)
$\varnothing_n$: Numerical Heat flux, (W)
χ^2: Squared Error

1. Introduction

The rise of micro/nanotechnology has promoted investigations into nanoscale heat transfer and the thermal properties of materials in semiconductors and electronics [1]. Scanning Thermal Microscopy (SThM) emerges as a vital tool for exploring nanoscale thermal characteristics. Key materials, like Silicon Dioxide (SiO_2), play a crucial role in materials science due to their diverse applications. SiO_2, widely used in microelectronics, optics, and insulation, relies on its thermal conductivity for usability [2]. SThM proves effective in examining polymers with lower thermal conductivity, offering a versatile approach compared to metals. The thermal probe, especially the Wollaston probe, is integral, functioning as both heat source and sensor, allowing simultaneous thermal and topographical imaging. Incorporated into a Wheatstone bridge circuit, it facilitates precise thermal measurements with sub-micrometer resolution.

Understanding SiO_2's thermal behavior is critical for managing heat in microelectronics and optimizing thermal barrier coatings. Fabrication methods influence SiO_2 film thermal conductivities, with this study focusing on low-pressure chemical vapor deposition. For this type of deposition, there exists limited research that evaluates thermal conductivities. Various

https://doi.org/10.25855/SFT2024-039

techniques, including plasma-enhanced chemical vapor deposition, are employed to determine SiO_2 thermal conductivity. Researchers, like Callard et al [3], utilize scanning thermal microscopy for examining silicon dioxide films, revealing intrinsic thermal conductivity. Other studies, such as Huang et al [4], utilize the micro-Raman method for noncontact measurements of thermal conductivity in thin films, providing valuable observations. The article is divided into three sections introducing scanning thermal microscopy, detailing the methodology for evaluating silicone dioxide's thermal conductivity, and presenting the obtained results with corresponding thermal analyses and numerical models.

2. Scanning Thermal Microscopy

SThM is a powerful technique used to measure and map thermal properties at the nanoscale and microscale. It involves scanning a thermal probe, which has its own resistive element depending on the type of probe used, over a sample surface to detect variations in temperature. These variations are highly dependent on the material's thermal conductivity, whether it is high or low.

2.1 Experimental Setup

To explore the Scanning Thermal Microscopy, which is based on the AFM (Atomic Force Microscopy) principle, the aim is to measure the local thermal conductivity or temperature variations of a sample's surface at the nanoscale. The AFM is a technique used in nanotechnology and surface science to visualize and manipulate matter at the atomic and molecular levels by scanning a probe over a surface. It provides high-resolution topographical information. In the SThM, the classical probe is replaced by a thermal-resistive probe in our case. This probe is inserted in a Wheatstone bridge and a feedback loop mechanism of the thermal control unit contributes to maintaining a constant temperature of the probe during the scanning process. As the probe encounters variations in thermal properties across the sample, changes in electrical resistance occur, providing insights into the local thermal characteristics. This technic allows for simultaneous topographical and thermal imaging.

Experimental measurements were conducted under ambient conditions. In this imaging technique, the thermal probe functions as a resistive heater, operating in conductivity contrast mode to enable the simultaneous acquisition of topographical and thermal images at the micro/nanoscale level. By applying a direct current of 50 mA through the resistive element via the Joule effect, the probe serves a dual purpose as both a heat source and a sensing component. Upon contact with the sample, the probe provides implicit information about the dissipated heat flux from the probe to the sample. This information is manifested as the required voltage to maintain a constant temperature of the probe while scanning the surface of the sample. The transmitted heat flux toward the sample is influenced by parameters such as the sample's thermal properties as its thermal conductivity. To mitigate the influence of water meniscus, the tip temperature was maintained at 100°C throughout this study [5].

2.2 Thermal resistive probe

In this study, we utilized a Wollaston microprobe [6] manufactured by the Czech Metrology Institute (CMI), in constant temperature mode to extract heat information from the studied sample. The probe’s thermal resistive element is created through electrochemical etching and bent into a V shape at its tip (figure 1). Composed of 90% platinum and 10% rhodium, the wire has a diameter of 5 μm, a length of 125 μm, and a curvature radius of 15 μm.

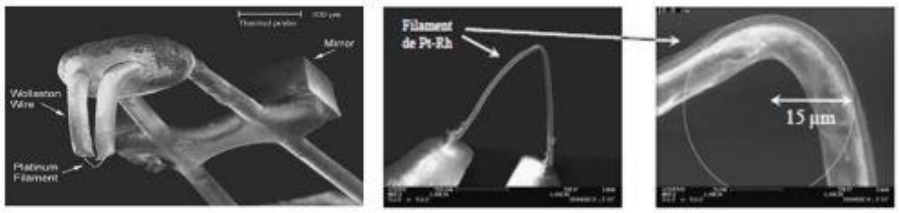

Figure 1: Wollaston thermal probe [7]

2.3 Silicone dioxide sample representation

The nanoscale thermal conductivity of silicon dioxide, our laboratory proposed a sample geometry that was fabricated by VTT/Finland as part of the QuantiHeat Project [8]. This sample features a triangular-shaped silicon dioxide step deposited on a silicon substrate and covered with polished CVD SiO_2 (refer to the figure 1). The sample is covered with a thin layer of silicon dioxide, we assume that the contact remains the same as we scan along its surface. The purpose behind this sample geometry is to achieve varying thicknesses of silicon dioxide within a single sample structure, allowing for the evaluation of local thermal information for this material. Since the sample is covered with a thin layer of silicon dioxide, we assume that the contact remains the same as we scan along its surface. The SiO_2/Si layer interface is linear, with an adjustable thickness ranging from 400 to 2150 nm. Initial experimental measurements were conducted to compare with a model describing heat transfer in the probe-sample system. This comparison enables the assessment of local thermal conductivity for SiO_2 thin films at different thicknesses varying between 500 and 1810 nm, specific to this sample geometry, through the application of inverse techniques.

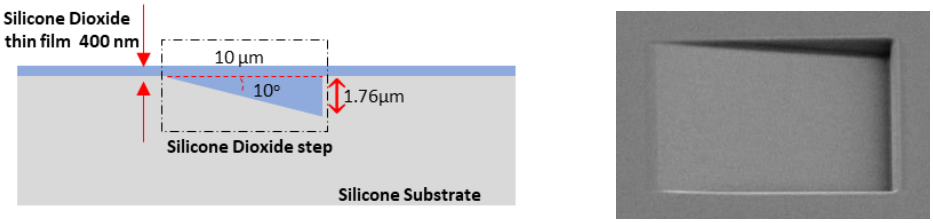

Figure 2: a) Sample structure b) Top view of Si by SEM

3. Methodology

3.1 Probe measurement illustration

As mentioned earlier, the first stage involved scanning the surface of the sample under normal ambient temperature conditions. The resulting thermal image (refer to Figure 3) is complemented by an electrical profile that offers detailed thermal information about the sample. It should be noted that this electrical profile is the key element in determining the heat transfer across this sample, complemented by a numerical model that considers the heat transfer modes.

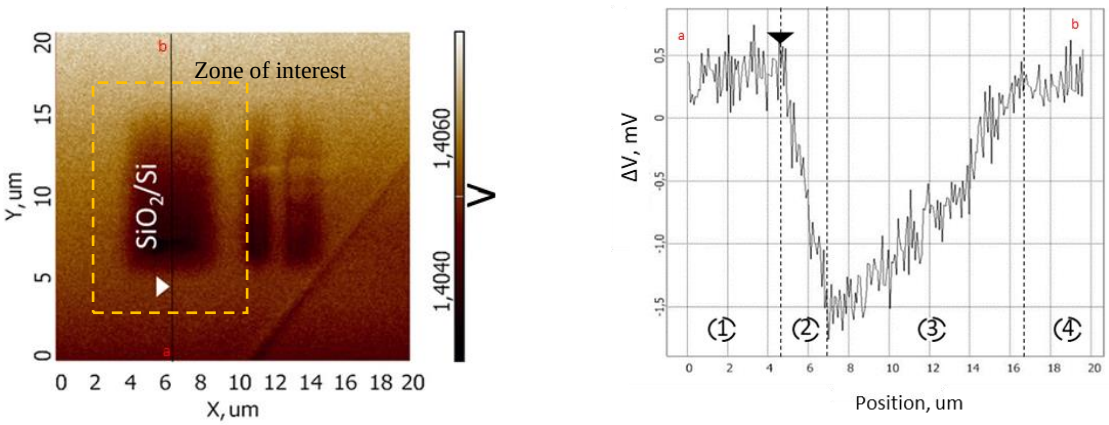

Figure 3: a) Thermal image and b) Experimental thermal profile along line ab

The transfer of heat from the probe to the sample reveals four distinct zones. Initially (zone 1), as the probe scans a constant SiO_2 thickness, the electrical signal remains constant. As the probe nears the edge of the triangle (zone 2), a noticeable decline in the output voltage is observed, attributed to a decrease in heat flux from the probe to the sample, indicating an increase in the SiO_2 layer thickness. In zone 3, the electrical signal rises due to a reduction in the SiO2 layer thickness. Subsequently, as the probe traverses a uniform SiO_2 layer thickness (zone 4), the electrical signal stabilizes, indicating a sustained dissipated heat flux. The value of thermal conductivity for the silicone substrate is about 130 W/m·K.

The variation in the electrical signal is attributed to power dissipated through the Joule effect and the establishment of thermal equilibrium of the probe. This understanding is crucial as it provides the experimental transmitted heat flux to the sample, enabling a comparative analysis with numerical heat fluxes to determine the corresponding thermal conductivity. The transition from the non-contact to the contact state corresponds to the total heat flux dissipated in the sample, which can be determined through the measurement of probe voltage. It should be noted that when working with low currents in the order of mA, the electrical signal tends to be noisy without affecting the reflected thermal/electrical information. Simultaneously, the calculation of the dissipated power through the platinum rhodium filament, both in contact and without contact configuration, is expressed through the following equations

$$P_c = \mathrm{Vout_c} \times \mathrm{Ip_c} - \mathrm{Vout_{wc}} \times \mathrm{Ip_{wc}} \quad (1)$$

$$P_{wc} = \mathrm{Rpt} \times (\mathrm{Ip}^2 - \mathrm{Ip_{wc}}^2) \quad (2)$$

The discrepancy in electrical power dissipation within the probe during the transition from a non-contact to a contact state is equal to the numerical heat flux dissipated in the sample, represented by the difference between the power in contact and out-of-contact configurations.

3.2 Model Approach

Three dimensions Finite Element Method (FEM) models were developed within COMSOL Multiphysics to enhance the precision of material thermal property characterization via scanning thermal microscopy [9]. This necessitated a dual-model approach, each focusing on distinct aspects of heat transfer. The first approach considers the probe in its entirety to

evaluate an equivalent heat transfer coefficient that accounts for losses through the probe holder. This coefficient will be implemented in the second model, which considers the probe-sample system. Both models account for numerous factors detailed in Al Alam's thesis [9].

The numerical representation of the probe's response in contact with the sample employs a thermo-electrical coupling approach. This involves the application of heat transfer and electric current equations in the finite element method. The heat transfer equation is solved for the resistive element, heated by the Joule effect, allowing the evaluation of the exchanged heat flux from the probe to the sample upon contact. The support structure of the probe, comprising two cylindrical disks, and the V-shaped wire composed of Platinum-Rhodium, are modeled based on their realistic dimensions and material composition. In the numerical model, all thermal properties for the Wollaston probe, silicon dioxide, and silicone materials are defined. Figure 4(a) represents the probe/sample model, including all imposed boundary conditions. After solving the heat transfer equations in steady state mode and evaluating the heat flux flowing from the probe to the sample at each probe position with respect to the sample the following numerical profile is obtained.

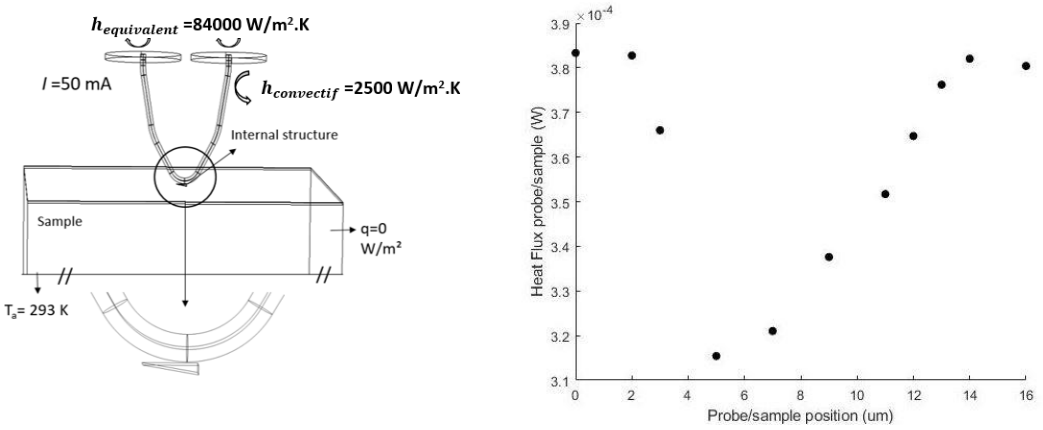

Figure 4(a): Probe/sample developed model Via FEM [9], (b)Thermal profile obtained by FEM.

Through a comparative analysis between the experimental thermal profile, as illustrated in Figure 3b, and the heat transfer profile derived from our computational model, we have successfully replicated the observed experimental behavior. In Figure 3b, the thermal profile obtained from experimental measurements using the Wollaston probe is presented. Meanwhile, Figure 4(b) showcases the corresponding thermal signal generated through Finite Element Method simulations. The finite element model plays a crucial role in understanding the experimental thermal profile regarding heat transfer modes within the surrounding air, the probe holder, and the sample. The FEM simulation involved a sequential computation of each point along the curve, in which the probe's positions above the sample surface were systematically varied. The thermal signal captured by the Wollaston probe demonstrated sensitivity to variations in thermal properties within the scanned volume. As the probe scanned the sample surface line by line, the thermal signal exhibited changes in heat transfer dynamics based on the specific area being scanned. This behavior signifies that the resulting thermal signal reflects information based on the scanned volume. Remarkably, this finding remains consistent for both numerical simulations and experimental observations, validating the accuracy of our modeling approach in capturing the complexities of nanoscale heat transfer. Building upon this accomplishment, our next initiative will involve the development

of an inverse method, enabling the determination of SiO_2 thermal conductivity. By contrasting the provided data with our constructed model, this method will enable us serving from those thermal information's to determine thermal conductivity for SiO_2 at different thicknesses.

3.3 Levenberg Marquardt

The assessment of thermal conductivity in thin film materials holds an importance in the domain of scanning thermal microscopy. In this study, we incorporate the inverse technique to determine the thermal conductivity of such materials. The dissipated heat flow is identified as the primary concern and is connected to an independently formulated inverse method, revolving a single variable—the thermal conductivity of SiO_2 material. This linkage aims to deduce the requisite thermal conductivity of the material by comparing the experimental and numerical heat transfer data. Various methodologies, including the Levenberg-Marquardt approach, the sequential estimation method, and the conjugated gradient method, are accessible to handle the complications of the inverse problem [10].

In this specific work, the Levenberg-Marquardt algorithm is employed for evaluating the thermal conductivity of nanostructured samples and thin film materials. This algorithm employs the sensitivity vector to guide updates, ensuring more efficient convergence in estimating the thermal conductivity parameter. By combining the strengths of the gradient descent and Gauss-Newton methods, the Levenberg-Marquardt approach addresses nonlinear least squares problems encountered in fitting mathematical models to observable data points. The aim is to reduce the error between the actual data points and the predicted values generated by our model. This is a standard objective when working with nonlinear parameters in mathematical models.

The Levenberg-Marquardt algorithm initiates with an initial parameter guess and iteratively refines these values to minimize the objective function. Its pivotal feature lies in dynamically adjusting the step size during each iteration based on the local behavior of the objective function. The algorithm adapts the damping factor throughout the iterations, behaving more like the gradient descent method when parameters are far from their optimal values, and transitioning to the Gauss-Newton method as parameters approach their optimal values [14-16]. This dynamic adjustment ensures rapid convergence in early iterations and precise local updates as the optimization progresses.

The weighting matrix is defined as an identity matrix under the assumption that there is no noise in the measurement data. In this case, the Squared error is calculated by:

$$\chi^2 = \sum_{i=1}^{i=m} [\Delta P - \emptyset_n]^2 \quad (4)$$

A thorough breakdown of the Levenberg-Marquardt algorithm, aimed at evaluating the thermal conductivity of Silicone Dioxide, is outlined in the figure 6.

4. Results

The assessed thermal conductivities for SiO_2 offer distinguished perspectives into the material's heat-conducting properties, presenting distinct values for varying SiO_2 layer thicknesses as displayed in figure 7.

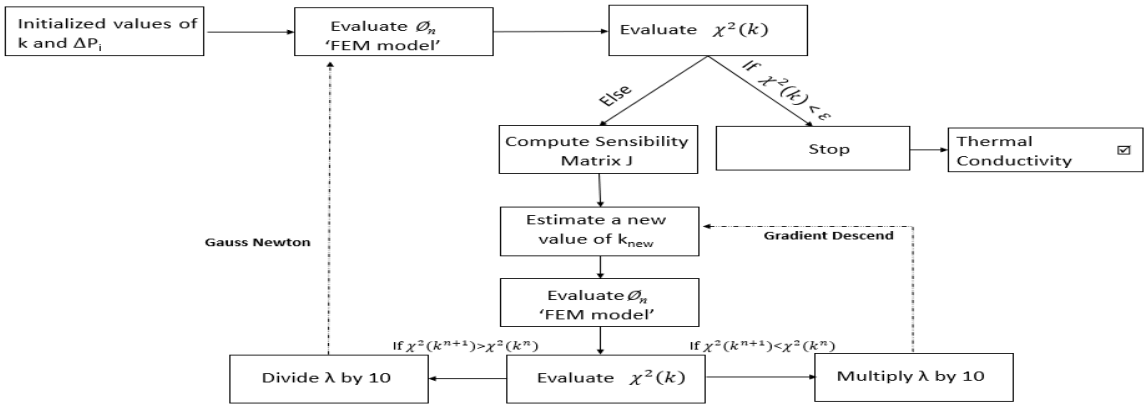

Figure 6: Levenberg-Marquardt algorithm

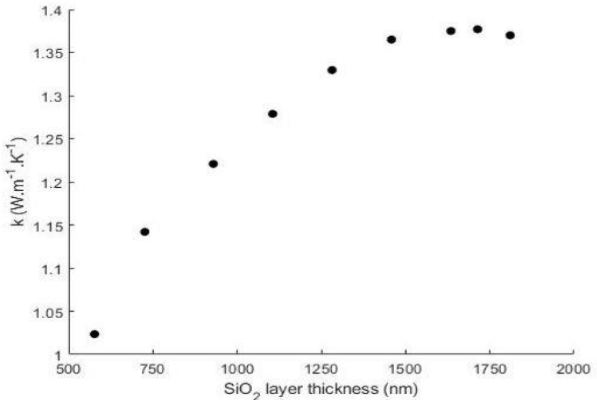

Figure 7: Evaluated thermal conductivity using inverse methods

As the SiO_2 layer gets thinner, its thermal conductivity decreases. This matches our expectations, as thinner layers usually have more heat conductivity due to increased scattering at their boundaries and less efficient phonon transport. The thickest SiO_2 layer, measuring 1810 μm, demonstrates the highest thermal conductivity at 1.38 W/m.K, while the thinnest layer, at 576 μm, records the lowest thermal conductivity at 1.02 W/m.K.

In addition to thermal conductivity values, the squared error from the Levenberg-Marquardt algorithm is pivotal for model validation. This error assesses the alignment between observed heat transfer quantities (ΔP) and numerically computed values $\emptyset_n$, demonstrating the effectiveness of the proposed methodology.

Our analysis yields squared error values ranging from 6.46E-09 to 2.04E-07, indicating a high level of accuracy in our model's predictions. Smaller squared errors signify a better match between observed and predicted heat transfer quantities. Notably, the SiO_2 layer with a thickness of 576.3 μm stands out with the smallest squared error of 6.46E-09, showcasing agreement between observed and predicted heat transfer quantities. Other SiO_2 layer thicknesses also exhibit relatively low squared errors. Furthermore, this value aligns with that of the few studies targeting the evaluation of the thermal conductivity of silicon dioxide in LPCVD. Yamane et al. [11] evaluated it at 475 nm to be approximately 0.95 W/m·K. The successful fit between the model and experimental data, demonstrated by minimal squared errors, highlights the efficacy of the employed Levenberg-Marquardt algorithm. It accurately

captures data trends, validates our model, and provides accurate estimates of SiO_2 thermal conductivity for LPCVD deposition across different thicknesses.

5. Conclusion

This investigation shows the effectiveness of a Wollaston microprobe in SThM and demonstrates its importance in understanding heat transfer at the nanoscale. The FEM models, based on a dual-model strategy, successfully capture the complexities of heat transfer within the probe-sample system, validated by experimental observations. The utilization of the Levenberg-Marquardt algorithm emerges as a robust method for determining thermal conductivity, yielding coherent results. The resulting trend of thermal conductivity, which varies with the variation of SiO_2 layer thickness, contributes to a better understanding of heat transfer in nanostructured materials. The minimal squared error values highlight the precision of the model, demonstrating the potential of the developed inverse technique for thermal conductivity determination. This thorough approach shows potential for using similar methods to study thin film materials by scanning thermal microscopy.

References

[1] A. Hammiche, H. M. Pollock, M. Song, D. J. Hourston, Sub-surface imagingby scanning thermal microscopy, Meas. Sci. Technol. 7, 142-150 (1996).

[2] A. Majumdar, M. Chandrachood, J. Lai, O. Nakabeppu, Y. Wu, Z. Shu, Thermal imaging by atomic force microscopy using thermocouple cantilever probes, Rev. Sci. Instr. 66-6, 3584-3592 (1995).

[3] S. Callard, G. Tallarida a, A. Borghesi, L. Zanotti, thermal conductivity of SiO2 by scanning thermal microscopy, Journal of Non-Crystalline Solids 245, 203-209, (1999).

[4] Z. Huang, Z.Tang J. Yu, S.Bai, thermak conductivity of amorphous and crystalline thin films by molecular dynamics simulation, Physica B 404, 1790–1793, (2009).

[5] A. Assy, S. Gomès Temperature-dependent capillary forces at nano-contacts for estimating the heat conduction through a water meniscus, Nanotechnology, 26, (2015).

[6] A. Majumdar, J. P. Carrejo, and J. Lai, Thermal imaging using the atomic force microscope. Appl. Phys. Lett., vol 62, (1993).

[7] O. Raphael, Contribution à la microscopie thermique à sonde locale en mode alternatif : Caractérisation de la réponse et de l'interaction sonde échantillon, (2008).

[8] https://cordis.europa.eu/project/id/604668/fr.

[9] P. Al Alam, Microscopie thermique à sonde locale : vers une analyse thermique des nanomatériaux, PhD thesis, University of Reims Champagne Ardenne, (2018).

[10] K. Madsen, N.B. Nielsen, and O. Tingleff. Methods for nonlinear least squares problems. Technical Report. Informatics and Mathematical Modeling, Technical University of Denmark, (2004).

[11] T. Yamane, N. Nagai, and S. Katayama, Measurement of thermal conductivity of silicon dioxide thin films using a 3ω method, J. Appl. Phys. 91, 9772, (2002).

Acknowledgements

The authors gratefully acknowledge the financial support provided by the European Union for the funding of the samples through the European Union Seventh Framework Programme FP7-NMP-2013-LARGE-7 under grant agreement no. 604668 (QuantiHeat project).